



## **NOISE REDUCTION OF A CENTRIFUGAL PLENUM FAN WITH LEADING-EDGE OR TRAILING-EDGE SERRATIONS**

Ignacio ZURBANO-FERNÁNDEZ<sup>1,2</sup>, Alain GUÉDEL<sup>1</sup>,  
Mirela ROBITU<sup>1</sup>, Michel ROGER<sup>3</sup>

<sup>1</sup> CETIAT, 25 avenue des Arts, B.P. 2042,  
69603 Villeurbanne cedex, France

<sup>2</sup> Univ Lyon, Ecole Centrale de Lyon, INSA Lyon, Université Claude  
Bernard Lyon I, CNRS, Laboratoire de Mécanique des Fluides et  
d'Acoustique, UMR 5509, 36 Avenue Guy de Collongue,  
F-69134, Écully, France

### **SUMMARY**

In this study, the application of leading-edge and trailing-edge serrations to the blades of a plenum fan is presented. RANS simulations on a non-serrated baseline impeller and design criteria for fixed airfoils have been used to design three impellers with leading-edge serrations and three with trailing-edge serrations. Leading-edge serrations have yielded a moderate sound power reduction (up to 1 dBA reduction in the overall sound power level) and only for some configurations. Trailing-edge serrations reduced broadband noise for all operating points and impeller prototypes (overall sound pressure decrease between 1 and 5 dBA). Leading-edge serrations reduce noise for low to mid frequencies but increase it over 1 kHz, whereas trailing-edge serrations reduce noise on the whole spectrum.

### **INTRODUCTION**

The numerical study of leading-edge serrations started as a means to delay stall on axial fans [1]. Corsini *et al.* [2] found numerically that this was achieved by the formation of a low-pressure core on the blade-suction surface at the trough of each serration. Zenger *et al.* [3] added serrations to the leading edge (LE) of the blades of an axial fan. The results showed a reduction in low-frequency broadband components (implying a reduction of unsteady forces), as well as in tonal components. Krömer *et al.* [4] tested both single and double-sine serrations on the LE of an axial fan, with the former being more efficient than the latter. Serrations with high  $2h$  and low  $\lambda$  (where  $2h$  and  $\lambda$  are respectively the amplitude and wavelength of the serrations, see Figure 2) are more efficient, with a noise reduction of 2 to 7 dB depending on the operation point. It seems that noise reduction is more influenced by changes on  $\lambda$  than  $2h$ .

Biedermann *et al.* [5] also added serrations to the leading edge of an axial fan. A maximum noise reduction of 13 dB was achieved for a certain configuration (but it also increased noise up to 3 dB at other operating points). It was observed that the noise reduction increases with bigger values of the serration wavelength and amplitude. An interesting parameter is the ratio  $\lambda/2h$ : high values yield the best noise reduction performance, but it rapidly degrades when we move away from the best efficiency point; low values of the ratio generate more stable noise reductions at various operating points. Double-amplitude serrations were also assessed, but they only showed small positive results on air performance and no impact on noise reduction, when compared with simple serrations.

Trailing edge serrations have also been applied to rotating machines, especially to wind turbines. Braun *et al.* [6] achieved a maximum noise reduction of 3.5 dB, also inducing a noise increase at high frequencies. Oerlemans *et al.* [7], added serrations to the trailing edge of a turbine blade, yielding an average noise reduction of 3.2 dB, with a slight noise increase (1-2 dB) over 1 kHz.

Weckmüller & Guérin [8] optimized trailing edge serrations on the front-rotor of a contra-rotating open rotor, yielding a reduction of only 0.2 dB on the tonal interaction noise. Another optimization on the same rotor [9] showed that tonal interaction noise could be reduced by 1 dB due to destructive interference in the radial direction, with longer serrations generating better results.

Lee *et al.* [10] simulated a ceiling fan with different serration geometries. An overall noise reduction of 9.2 dB was predicted with flat serrations, 4.7 with sawtooth, 10.9 with rectangular, 13.9 with half flat tip (only the outer half of the blade is serrated) and 5.0 with half rectangular half flat tip. However, when tested experimentally, a reduction of only 4.1 dB(A) was measured with half flat tip serrations. Pagliaroli *et al.* [11] added serrations to the trailing edge of a UAV propeller. Broadband noise reduction was achieved at low frequencies, but the aerodynamic performance of the propeller was degraded (and noise increase was observed at certain angles). Noise reduction is highly directional.

Previous experimental and numerical studies were conducted with leading-edge or trailing-edge serrations on axial fans, wind turbines and drones. However, up to this day, only leading-edge serrations had been used on a plenum fan, on a paper presented by the same authors of the current study [14]. This paper complements the previous results and applies for the first time trailing-edge serrations to a plenum fan.

## PROTOTYPE DESIGN: LEADING-EDGE SERRATIONS

Several design criteria from airfoils were used to dimension the serrations: [5, 12, 13]. The design process has already been described in [14]. To sum up, the integral turbulence lengthscale  $L$  is estimated with CFD RANS simulations. This value is then used to calculate the optimum serration angle, according to the equation in [12],  $\varpi_{opt} = \tan^{-1}(2h/L)$ . The predicted optimum serration configuration has a wavelength of  $\lambda = 16 \text{ mm}$  and an amplitude of  $2h = 22 \text{ mm}$ . The blades of the baseline plenum fan have been modified with leading-edge serrations with these values. To perform a study on the influence of the serration geometry, in terms of  $2h$  and  $\lambda$ , two other prototypes have been designed. In one case,  $\lambda$  has been doubled while keeping the same  $2h$ . In the other,  $2h$  is twice as big while maintaining the same  $\lambda$ . The parameters for the three impellers are summarized in Table 1. The ratio  $\lambda/2h$  has been added because it is commonly used to describe the sharpness of the serrations.

Table 1: Leading-edge serration parameters

Designation	$\lambda$ [mm]	$h$ [mm]	$\lambda/2h$
LE_L8H11	8	11	0.36
LE_L16H11	16	11	0.73
LE_L16H22	16	22	0.36

The manufacturing of the prototypes, carried out by the company Ziehl-Abegg SE, was similar to that of the baseline fan, without serrations. The only modification is the removal of material to carve the serrations on the blade. This has been done with a laser-cutting tool; the blade surface area is slightly reduced, and thus is expected to have an impact on the blade lift and implicitly on the fan curve. This potential degradation of the fan performance will be considered in the comparison of the acoustic results of the different blade geometries by using the specific noise level (see Equation 1). Figure 1 shows the prototypes with serrated leading edges.



Figure 1: Prototypes of impellers with leading-edge serrations

## PROTOTYPE DESIGN: TRAILING-EDGE SERRATIONS

Trailing-edge serrations are also defined based on results on airfoils. For the serration amplitude  $2h$ , Gruber [15] proposed that at least  $h > 0.25\delta$ , where  $\delta$  is the boundary layer thickness should be considered. The value of  $h = 2\delta$ , proposed by Arce León *et al.* [16], has been taken as a reference. As  $h$  should be as big as possible, the maximum value of  $\delta$ , estimated from CFD simulations of the baseline impeller, has been considered (see [14]). It has been rounded to 8.5 mm, so  $h = 2\delta = 17mm$ .

Gruber [15] also proposed that the relationship between serration wavelength and amplitude should be  $\lambda < 2h$ , and it was also suggested that a value of  $\lambda < h/6.5$  should yield even better results. If this extreme criterion was applied in our case, it will yield a wavelength of 2.6 mm, which is extremely small. As a compromise, a value of  $\lambda = 4 mm$  has been used. A third design criterion regarding the serration shape has been incorporated into the design. Ragni *et al.* found [17] that "iron-shaped" serrations can reduce up to 2 dB with respect to conventional sawtooth serrations in the range  $5 < St < 15$  (here  $St$  is the chord-based Strouhal). This geometry has been selected for the serration design (see Fig. 2).

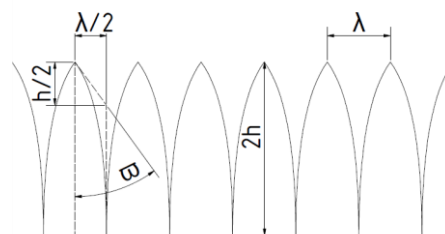


Figure 2: Iron-shaped serrations

As it has been done for leading-edge serrations, two other impeller prototypes have been manufactured, with one of the parameters ( $2h$  or  $\lambda$ ) being modified at a time. It is to be noted that, as the angle of the serration valley is very narrow, the laser-cutting tool used for manufacturing could not cut all the way through. Therefore, the effective amplitude  $h_e$  is shorter than the design amplitude  $h$ . Table 2 presents the main parameters of the impellers, which are shown in Figure 3. Again, the  $\lambda/2h$  ratio, albeit redundant, has been included for the sake of completion.

Table 2: Trailing-edge serration parameters

Designation	$\lambda$ [mm]	h [mm]	$h_e$ [mm]	$\lambda/2h$
TE_L4H12	4	17	12	0.17
TE_L8H12	8	17	12	0.33
TE_L8H8	8	11	8	0.5



Figure 3: Prototypes of impellers with trailing-edge serrations

## EXPERIMENTAL SETUP

All impeller prototypes and the baseline fan have been tested in a double reverberant room according to test category A: non-ducted at inlet and outlet (see Figure 4). The fan is mounted on a support, on the partition between the two rooms of different sizes, the bigger room being on the inlet side. An auxiliary fan allows adjusting the operating point of the test fan. The flowrate is measured with a multi-nozzle chamber while the fan pressure is obtained according to ISO 5801 [18] with pressure rings in both reverberant rooms. The fan sound pressure levels are determined in both rooms following ISO 13347-2 [19], using a rotating microphone in the big room and 3 fixed microphones in the small one to make a spatial average of the sound pressure field in each room. The average sound pressure level measured inside each reverberating room allows us to deduce the sound power level of the fan in the room.

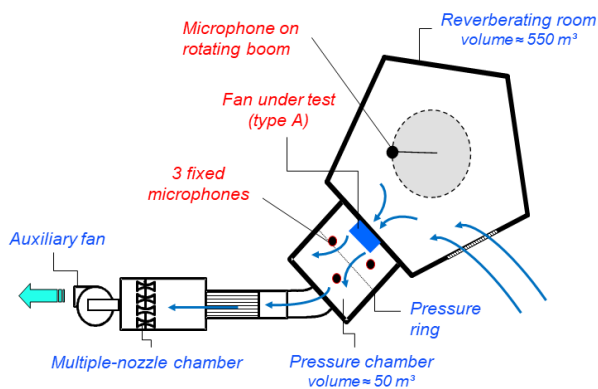


Figure 4: Top view layout of the test facility (left) and view of the outlet pressure chamber with the fan assembly (right)

For each prototype, the same assembly (base, inlet nozzle, motor as in Figure 4, right) has been used, with only the impeller being replaced. The motor is connected to a variable-frequency drive (VFD) which allows changing the speed from 1440 rpm (100 % of the nominal speed) to 720 rpm (50 % of the nominal speed). All the results have been converted to the target rotating speed (e.g., 1440 rpm for nominal speed) and an air density of  $\rho = 1.2 \text{ kg/m}^3$ , which are very close to the test values.

## RESULTS: LEADING-EDGE SERRATIONS

The fan aerodynamic curves for the baseline impeller and the three prototypes are shown in Figure 5 (left), where the fan total pressure  $p_f$  is plotted against the airflow  $q_v$ . For all the serration configurations there is a pressure decrease with respect to the baseline impeller at low flowrate, and a moderate pressure increase at high flowrate. In terms of pressure, the LE\_L16H11 impeller is the best, followed by LE\_L8H11 and LE\_L16H22. The same hierarchy (see Figure 5, right) is observed for the overall total efficiency ( $\eta_{ed} = p_f q_v / P_{ed}$ , where  $P_{ed}$  is the electric power measured at the inlet of the variable frequency drive).

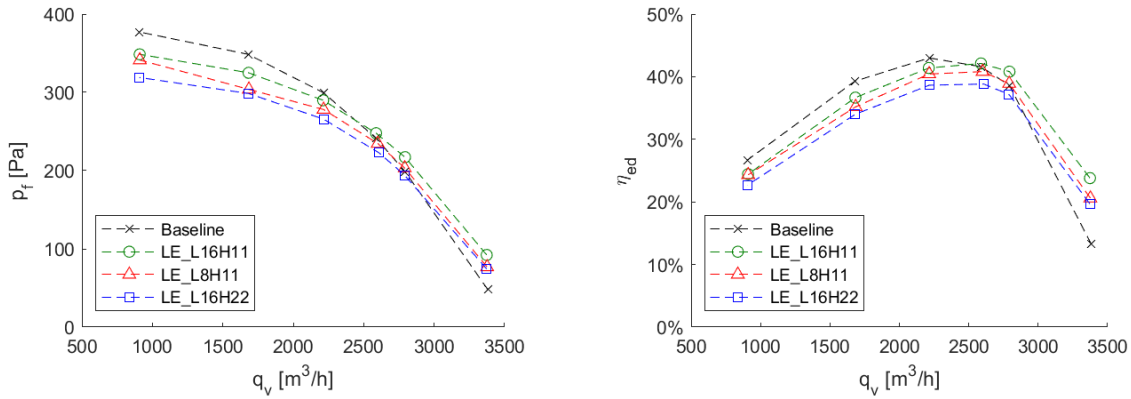


Figure 5: Fan total pressure (left) and overall efficiency (right),  $N=1440$  rpm

To account for the reduction in fan pressure due to serrations, the specific noise formula is used:

$$L_{p,spec}(f) = L_p(f) - 10 \log_{10}(q_v) - 20 \log_{10}(p_f) \quad (1)$$

where  $q_v$  is the airflow in  $m^3/h$  and  $p_f$  is the fan total pressure in  $Pa$ . The measured acoustic spectra show several peaks, some of which are multiples of the rotating frequency (excluding the blade passing frequency). It was found that most of them are induced by mechanical vibrations in the experimental setup, despite all rotors being balanced after manufacturing. As the focus of the present study is the aerodynamic broadband noise, a one-dimensional median filter, of order 14, was applied to the raw data to remove most of these peaks (see [20] for more details about the peaks and the filtering process). Then, the biggest of them, which have not been treated by the filter, have been trimmed manually. Finally, the specific noise is calculated. The result for the best efficiency point ( $q_v = 2196 m^3/h$ ) is shown in Figure 6 (left). The sound pressure level reduction  $\Delta L_p$  has also been obtained in Figure 6 (right). This is done by subtracting the serrated impeller spectrum from the baseline spectrum (see Equation 2):

$$\Delta L_p = L_{p,serrated\ impeller} - L_{p,baseline} \quad (2)$$

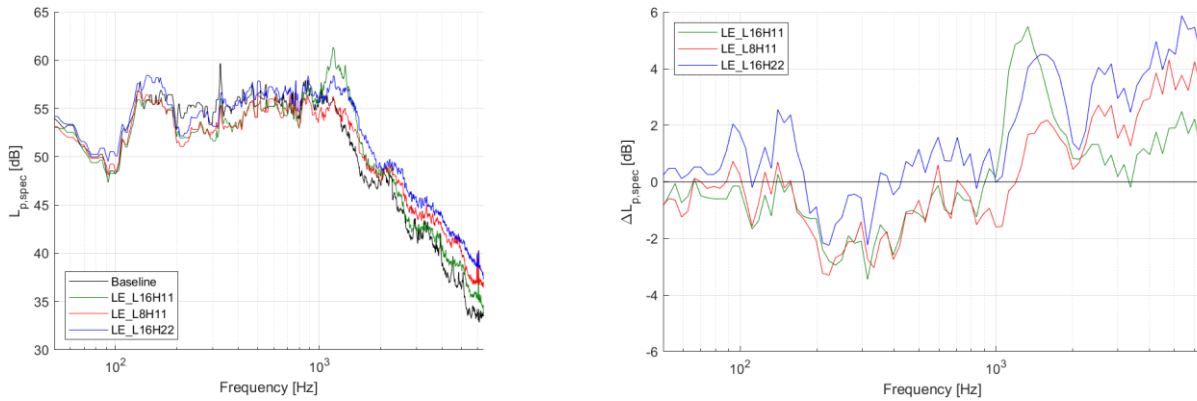


Figure 6: Filtered outlet specific noise for the best efficiency point,  $q_v = 2200 \text{ m}^3/\text{h}$ ,  $N=1440 \text{ rpm}$ : specific sound pressure level  $\Delta f = 2 \text{ Hz}$  (left); filtered specific sound pressure level reduction in 1/12th octave bands (right)

For the low frequencies (roughly under 1000 Hz), leading-edge serrations achieved a certain noise reduction. However, noise is increased at high frequencies. The sound pressure levels are integrated over the whole spectrum to obtain the overall level. Then, the A-weighting is applied. The results obtained, for both inlet and outlet noise levels, are shown in Figure 7. Leading-edge serrations do not appear to be an efficient means to reduce noise, for the three prototypes tested within this study. The specific noise is actually increased at most operating points. The only exception is the point of maximum flowrate ( $q_v = 3300 \text{ m}^3/\text{h}$ ), where there is a substantial specific noise reduction due to pressure recovery whatever the serration geometry.

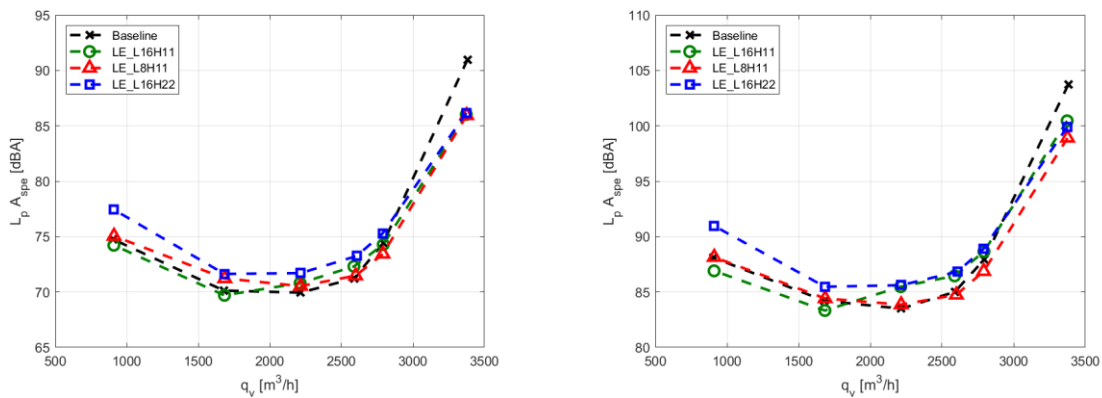


Figure 7: Overall specific sound pressure level, inlet (left) and outlet (right),  $N=1440 \text{ rpm}$

## RESULTS: TRAILING-EDGE SERRATIONS

The fan aerodynamic curves for the baseline fan and the three prototypes are shown in Figure 8 (left). In this case, there is a pressure drop for all the prototype configurations, with no pressure increase whatsoever. It is the same for the overall efficiency, depicted in Figure 8 (right).

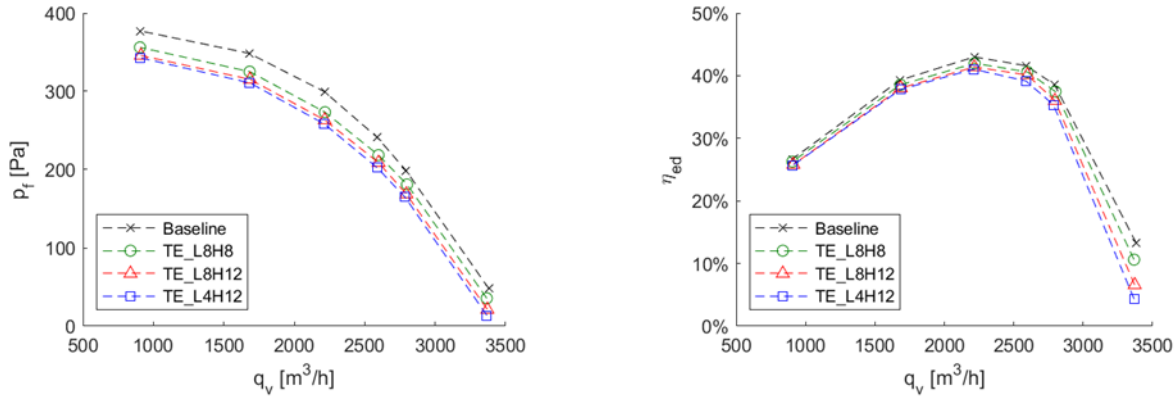


Figure 8: Fan total pressure (left) and overall efficiency (right),  $N=1440$  rpm

The specific noise spectrum for the best efficiency point ( $q_v = 2196 \text{ m}^3/\text{h}$ ) is shown in Figure 9 (left), after applying the same filtering algorithm used on the leading-edge serrations raw data. The noise reduction is broadband and more important for low and mid frequencies. The sound pressure reduction, calculated with Equation 2, is shown in Figure 9 (right).

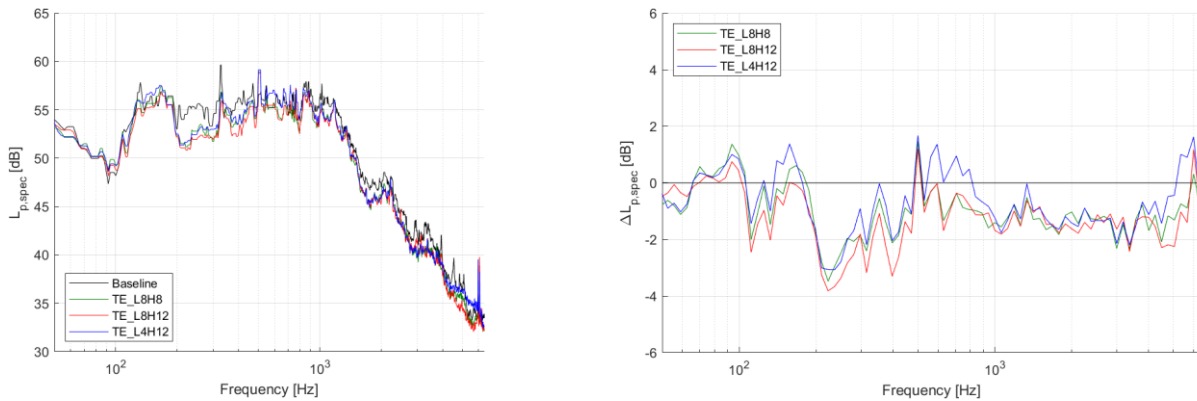


Figure 9: Outlet noise for the best efficiency point,  $q_v = 2200 \text{ m}^3/\text{h}$ ,  $N=1440$  rpm: specific sound pressure level  $\Delta f = 2 \text{ Hz}$  (left); filtered specific sound pressure level reduction in 1/12th octave bands (right)

The overall specific sound pressure levels for all operating points are shown in Figure 10. For some of them, a noise reduction between 1 and 3 dB(A) has been measured for all three impellers, with TE\_L8H12 slightly quieter than the other impellers. However, the impact of the change in serration geometry on the noise reduction is globally small for the tested configurations.

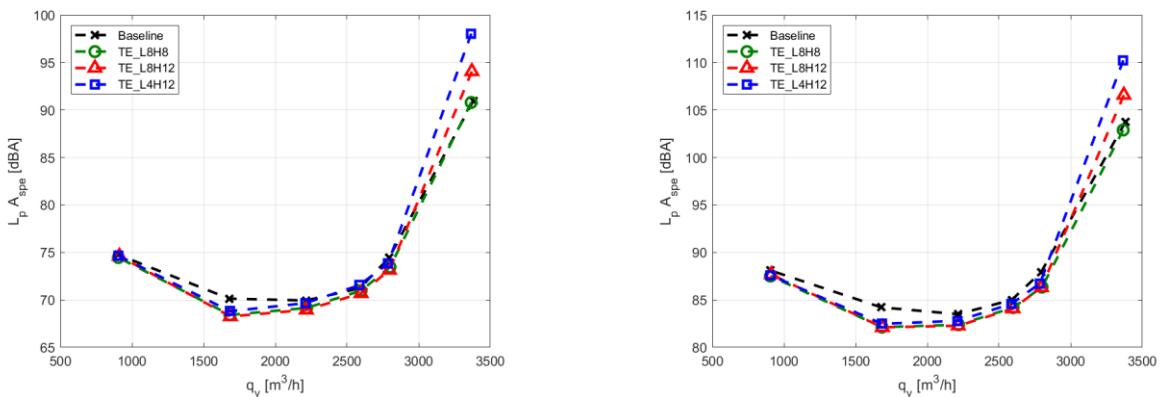


Figure 10: Overall specific sound pressure level, inlet (left) and outlet (right),  $N=1440$  rpm

An interesting result has been observed at 50 % of the nominal rotating speed (720 rpm). For the lower flow values, an important noise reduction has been observed, as shown in Figure 11 (left). This can be explained by analyzing the spectra for the flowrate  $q_v = 585 \text{ m}^3/\text{h}$ , displayed in Figure 11 (right). The spectrum of the baseline impeller shows a peak with a considerable emergence around 5000 Hz. Serrations highly reduce its amplitude (TE\_L8H8) or practically cancel it (TE\_L8H12 and TE\_L4H12). This peak might be due to laminar boundary layer vortex-shedding (LBL-VS), which disappears with some specific serration geometries.

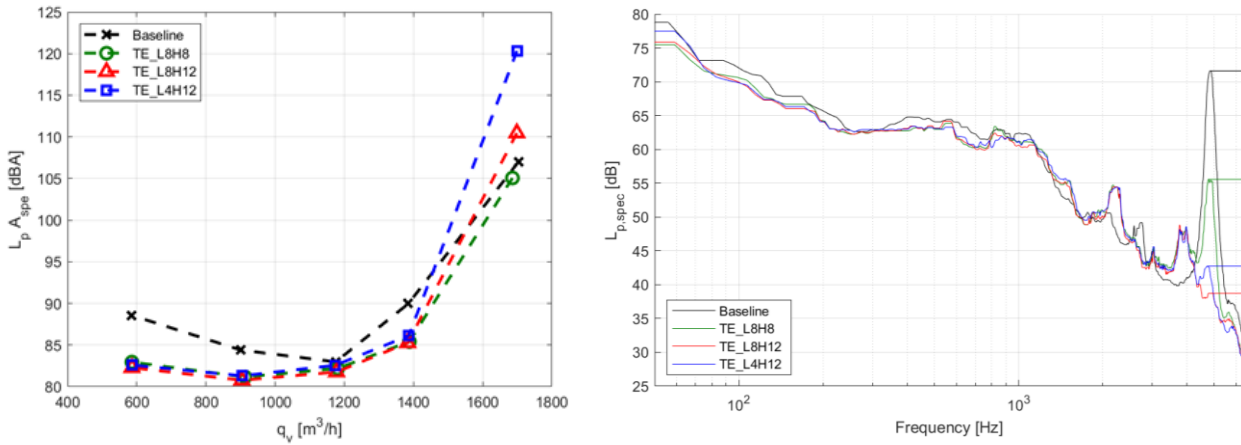


Figure 11: Overall outlet specific sound pressure level (left) and specific sound pressure (right), for 720 rpm and  $q_v = 585 \text{ m}^3/\text{h}$ .

Another element which supports the previous hypothesis is displayed in

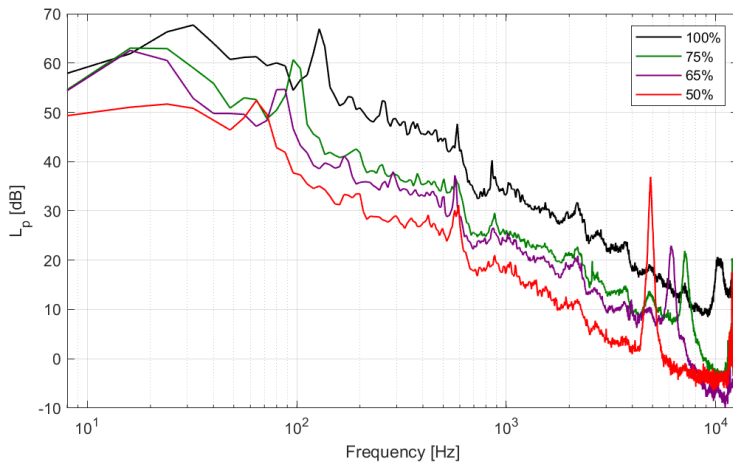


Figure 12. This plot shows the inlet noise of the baseline fan, for different rotating speeds at the same value of the dimensionless flow coefficient

$$\bar{\delta} = q_v/US \quad (3)$$

where  $U = \pi D_e N$  and  $S = \pi D_e L$ .  $D_e$  is the outer diameter (361 mm),  $N$  is the rotating speed and  $L$  is the outlet width (98 mm). When the rotating speed is reduced, the peak which appears roughly around 10 kHz at 100 % rotating speed is shifted towards lower frequencies and it increases in amplitude, scaling with the velocity. If we apply the following formula [21]:

$$f \cdot \frac{T}{U_e} \approx 1 \quad (4)$$

where  $T$  is the blade thickness (2 mm),  $f$  is the frequency, and  $Ue$  is the relative flow velocity outside the boundary layer (estimated from the CFD simulations [20]), it can be found that the LBL-VS peaks should be around 10 kHz, 7500 Hz, 6500 Hz and 5000 Hz for the rotating speeds of 100 %, 75 %, 65 % and 50 %, respectively. This is consistent with the presence of LBL-VS. Besides, if the noise is generated by a laminar instability, the reduction of the rotating speed could lead to an increase in the laminarity of the flow, therefore increasing the amplitude of the peak. The peaks could also be explained by other mechanisms, such as von Kármán vortex shedding, but the former hypothesis seems more likely. The addition of trailing-edge serrations would break down the vortices from the laminar instability, therefore mitigating or even completely cancelling this phenomenon.

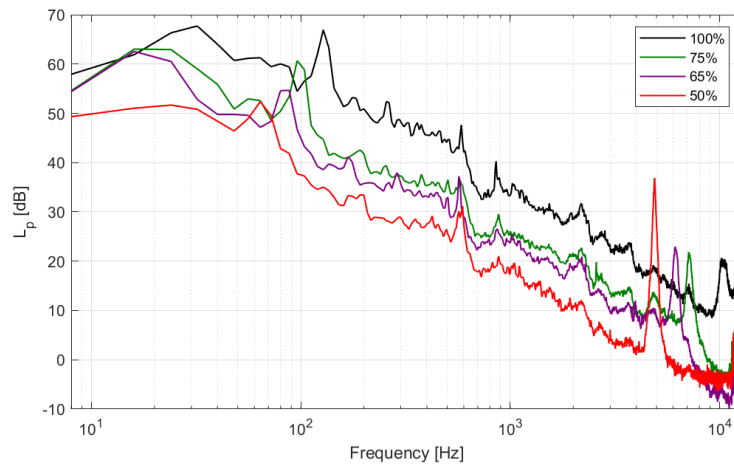


Figure 12: Inlet noise of the baseline fan for different rotating speeds,  $\bar{\delta}=0.1$

## CONCLUSION AND OUTLOOK

A design process for leading and trailing-edge serrations on a plenum fan has been carried out to reduce the noise. Six impeller prototypes with serrations were manufactured and tested to investigate their aerodynamic and acoustic effects. For both solutions, a certain degradation of the aerodynamic performance has been measured.

Leading-edge serrations tend to reduce the noise level under 1000 Hz but can increase the noise at higher frequencies, depending on the operating point. The impact on the overall sound level is rather limited and serrations actually increase the overall noise if we consider the degradation of the aerodynamic performance.

Trailing-edge serrations reduce noise for all frequencies at some operating points, with a maximum decrease of around 1-2 dB(A) at nominal speed. At low flow rate and low rotating speed, a substantial noise reduction of up to 8 dB(A) is observed due to the mitigation or even cancellation of a high-frequency peak. This peak, which also appears at higher speeds with a frequency shift, is most certainly due to a noise source located at the trailing edge and the most likely origin of this source points towards laminar boundary-layer vortex shedding, but this needs further validation.

All impeller prototypes have been designed and optimized to yield substantial noise reductions. The discrepancies between the measured and expected values could be due to the validity of the serration design criteria which may not be suited for this type of fan, as those criteria have mainly been assessed on stationary 2D airfoils in wind tunnels, or for the characteristics of the inlet turbulence close to the blade leading edge. Another explanation could be the existence of other noise sources. Trailing-edge noise seems to be dominant over leading-edge noise, but this may be a

consequence of an average moderate level of turbulence at the inlet. Furthermore, the addition of serrations may change the boundary layer in a way that generates more noise.

A better design strategy may have been to use the  $k-w$  SST turbulence model instead of  $k-e$ , as it is typically better suited for turbomachinery applications. Finally, we have used the same spanwise serration dimension for the sake of simplicity. Instead, the serration dimension could have been adapted to the spanwise evolution of the flow (turbulence for the LE, pressure fluctuations in the blade boundary layer for the TE), changing their amplitude and wavelength along the span. Another alternative would have been to add serrations only where they are needed the most, keeping the rest of the blade unchanged. This would allow reducing the blade surface loss due to the presence of serrations, and thus it would be expected to have an impact on the fan performance.

For the particular case of serrations on the leading edge, the estimation of the turbulence should have also included the curved part of the leading edge. Furthermore, the maximum turbulence length scale should have been used instead of the average length along the blade span. For the trailing-edge serrations, the next step could be the use of a more exotic serration geometry, such as ogee-shaped [22] or slits [23].

## ACKNOWLEDGMENTS

The authors wish to thank Hervé Bingan, Jean-Hugues Salazar and Benoît Savanier, from CETIAT, for their contribution to the tests; Hervé Miler, from CETIAT, for his help with the numerical simulations; and also Frieder Lörcher and Walter Angelis, from Ziehl-Abegg SE, for providing the baseline fan and manufacturing the fan prototypes.

The present work has received funding from the European Union's Horizon 2020 research and innovation program under the Marie Skłodowska-Curie SmartAnswer project (grant agreement No 722401). It has also received funds from CETIAT's industrial members which are fan manufacturers.

## BIBLIOGRAPHY & REFERENCES

- [1] Corsini, A., Delibra, G., and Sheard, A. G., *Leading edge bumps in ventilation fans*, Proceedings of the ASME Turbo Expo, **2013**. <https://doi.org/10.1115/GT2013-94853>
- [2] Corsini, A., Delibra, G., and Sheard, A. G., *On the Role of Leading-Edge Bumps in the Control of Stall Onset in Axial Fan Blades*, Journal of Fluids Engineering, Vol. 135, No. 8, **2013**, URL <https://doi.org/10.1115/1.4024115>
- [3] Zenger, F., Renz, A., and Becker, S., *Experimental Investigation of Sound Reduction by Leading Edge Serrations in Axial Fans*, 23rd AIAA/CEAS Aeroacoustics Conference, **2017**, URL <https://doi.org/10.2514/6.2017-3387>
- [4] Krömer, F., Westermeier, M., Renz, A., Becker, S., and Alexander, F., *Sound reduction by leading edge serrations in low-pressure axial fans*, FAN 2018 - International Conference on Fan Noise, Aerodynamics, Applications & Systems, **2018**.
- [5] Biedermann, T., Hintzen, N., Kameier, F., Chong, T. P., and Paschereit, C. O., *On the Transfer of Leading Edge Serrations from Isolated Aerofoil to Ducted Low-Pressure Fan Application*, AIAA/CEAS Aeroacoustics Conference, **2018**, URL <https://arc.aiaa.org/doi/10.2514/6.2018-2956>
- [6] Braun, K., Van der Borg, N., Dassen, A., Doorenspleet, F., Gordner, A., Ocker, J., and Parchen,

- R., *Serrated trailing edge noise (STENO)*, Proceedings of the European Wind Energy Conference, 1999, pp. 180–183. URL <http://books.google.dk/books?id=TGbZHwAACAAJ>.
- [7] Oerlemans, S., Fisher, M., Maeder, T., and Kögler, K., *Reduction of Wind Turbine Noise Using Optimized Airfoils and Trailing-Edge Serrations*, AIAA Journal, Vol. 47, No. 6, **2009**, pp. 1470–1481. URL <http://arc.aiaa.org/doi/10.2514/1.38888>
- [8] Weckmüller, C., and Guérin, S., *On the influence of trailing-edge serrations on open-rotor tonal noise*, 18th AIAA/CEAS Aeroacoustics Conference (33rd AIAA Aeroacoustics Conference), **2012**. <https://doi.org/10.2514/6.2012-2124>
- [9] Jaron, R., Moreau, A., Guérin, S., Schnell, *Optimization of Trailing-Edge Serrations to Reduce Open-Rotor Tonal Interaction Noise*, ISROMAC 2016 International Symposium on Transport Phenomena and Dynamics of Rotating Machinery, **2016**
- [10] Lee, H. M., Lim, K. M., and Lee, H. P., *Reduction of ceiling fan noise by serrated trailing edge*, Fluctuation and Noise Letters, Vol. 17, No. 3, **2018**, URL <https://doi.org/10.1142/S0219477518500268>
- [11] Pagliaroli, T., Camussi, R., Candeloro, P., Giannini, O., Bella, G., and Panciroli, R., *Aeroacoustic Study of small scale Rotors for mini Drone Propulsion: Serrated Trailing Edge Effect*, 2018 AIAA/CEAS Aeroacoustics Conference **2018**, URL <https://arc.aiaa.org/doi/10.2514/6.2018-3449>
- [12] Chaitanya, P., Narayanan, S., Joseph, P., Vanderwel, C., Turner, J., Kim, J., and Ganapathisubramani, B., *Broadband noise reduction through leading edge serrations on realistic aerofoils*, 21st AIAA/CEAS Aeroacoustics Conference, **2015**, URL <https://doi.org/10.2514/6.2015-2202>
- [13] Narayanan, S., Chaitanya, P., Haeri, S., Joseph, P., Kim, J. W., and Polacsek, C., *Airfoil noise reductions through leading edge serrations*, Physics of Fluids, Vol. 27, No. 2, **2015**, URL <https://doi.org/10.1063/1.4907798>
- [14] Zurbano-Fernández, I., Guédel, A., and Robitu, M., *Experimental investigation of the noise reduction of a plug fan by leading-edge serrations*, Proceedings of the 23rd International Congress on Acoustics, **2019**, URL <http://pub.dega-akustik.de/ICA2019/data/articles/001414.pdf>
- [15] Gruber, M., *Airfoil noise reduction by edge treatments*, Thesis for the degree of Doctor of Philosophy, University of Southampton, **2012**, URL <https://eprints.soton.ac.uk/349012/>
- [16] Arce Leon, C., Avallone, F., Pröbsting, S., and Ragni, D., *PIV Investigation of the Flow Past Solid and Slitted Sawtooth Serrated Trailing Edges*, **2016**. <https://doi.org/10.2514/6.2016-1014>
- [17] Ragni, D., Avallone, F., and van der Velden, W. C., *Concave serrations on broadband trailing edge noise reduction*, 23rd AIAA/CEAS Aeroacoustics Conference, **2017**, URL <https://arc.aiaa.org/doi/10.2514/6.2017-4174>
- [18] *ISO 5801: Performance testing using standardized airways*, **2017**, URL <https://www.iso.org/standard/39542.html>
- [19] *ISO 13347: Determination of fan sound power levels under standardized laboratory conditions — Part 2: Reverberant room method*, **2004**, URL <https://www.iso.org/standard/29753.html>
- [20] Zurbano-Fernández, I., *Reduction of the broadband noise of centrifugal fans used for HVAC in buildings*, Thèse de doctorat en acoustique, École Centrale de Lyon, **2021**, URL <http://www.theses.fr/2021LYSEC027>

- [21] Guédel, A., *Les ventilateurs : Bruit et techniques de réduction*, Paris, Dunod, **2015**, ISBN : 9782100725250
- [22] B. Lyu, L. Ayton, and P. Chaitanya. *Leading- and trailing-edge noise reduction using serrations of new geometry*, Proceedings of the 23rd International Congress on Acoustics, **2019**, URL <https://pub.dega-akustik.de/ICA2019/data/articles/001531.pdf>
- [23] F. Avallone, W.C van der Velden, D. Ragni, D. Casalino, *Noise reduction mechanisms of sawtooth and combed-sawtooth trailing edge serrations*, Journal of Fluid Mechanics 848, **2018**, pp. 560-591, URL <https://doi.org/10.1017/jfm.2018.377>

Distributed under the terms of the Creative Commons Attribution 4.0 International License (CC BY 4.0).  
<https://creativecommons.org/licenses/by/4.0/>